J|A|C|S
COMMUNICATIONS

Published on Web 04/19/2006

Hydrogenation and Hydrocarbonation and Etching of Single-Walled Carbon Nanotubes

Guangyu Zhang, Pengfei Qi, Xinran Wang, Yuerui Lu, David Mann, Xiaolin Li, and Hongjie Dai*

Department of Chemistry and Laboratory for Advanced Materials, Stanford University, Stanford, California 94305

Received February 23, 2006; E-mail: hdai@stanford.edu

Understanding the interactions between molecules and single-walled carbon nanotubes (SWNTs) is of fundamental and practical importance.[1] While weak adsorption of molecular hydrogen on SWNTs has been widely investigated and debated, covalent reactions between hydrogen and SWNTs are less explored. Only a handful experiments have been done at room temperature (rt) thus far with a main finding that SWNTs are hydrogenated by atomic hydrogen or hydrogen plasma with an atomic coverage up to ~65%.[2,3] It is also found recently that hydrogenation plays a role in affecting the growth of SWNTs in plasma-enhanced chemical vapor deposition.[4]

Here we present a systematic experimental investigation of the reactions between H-plasma and SWNTs at various temperatures. We reveal structural, infrared (IR), Raman spectroscopic, and electrical properties of hydrogenated SWNTs. Further, we uncover hydrogen-plasma cutting and etching of SWNTs and the nanotube diameter dependence of the etching effect.

We used a quasi *remote* radio frequency (rf) plasma system to generate H-plasma under a H_2 gas flow at 1 Torr and an rf power of 30 W. Chemical vapor deposition (CVD)[1,5] grown SWNTs on SiO_2 substrates were placed downstream of the plasma source (to avoid direct SWNT exposure to energetic plasma) and exposed to the H-radicals carried over by the gas flow (see Supporting Information).

Systematic atomic force microscopy (AFM) imaging reveals an apparent increase in the topographic heights of nanotubes on SiO_2 (Figure 1) after H-plasma treatment at rt for 3 min. The height increase is ~3 ± 1 Å based on measurements (Figure 1) over 100 nanotubes before and after exposure to H-plasma. We attribute this height increase to hydrogenation of the sidewalls of SWNTs. A covalently bonded H to the nanotube sidewall adds ~1 Å. Also, calculations have shown that hydrogenation of an SWNT lead to deformation and relaxation in the carbon network.[6] These are the likely causes to the observed nanotube size increase. Note that the height change appears uniform along the lengths of nanotubes, indicating dense hydrogenation sites (spacing of sites should be well below the AFM lateral resolution of ~5−10 nm). This is the first time that SWNT "swelling" is observed due to hydrogenation.

To further elucidate the hydrogenation of SWNTs, we have carried out IR spectroscopy measurements of dense vertically aligned SWNT films[4] before and after rt H-plasma treatment and subsequent stepwise thermal annealing up to 500 °C. After rt H-plasma treatment of the nanotubes, vibration bands in the range of 2750−3000 cm^{-1} with peaks centered at ~2850 cm^{-1} and ~2920 cm^{-1} are observed (Figure 2a). Tentatively, we assign the band centered at 2920 cm^{-1} to sp^3 CH stretching or asymmetric stretching of sp^3 CH_2 groups.[7] The 2850 cm^{-1} peak matches symmetric stretching of sp^3 CH_2. These suggest the formation of various $C-H_x$ species including sp^3 CH on the sidewalls and sp^3 CH_2 species likely at the defect sites and ends of SWNTs (abundant ends exist in our vertically aligned SWNTs). Upon thermal annealing, we observed

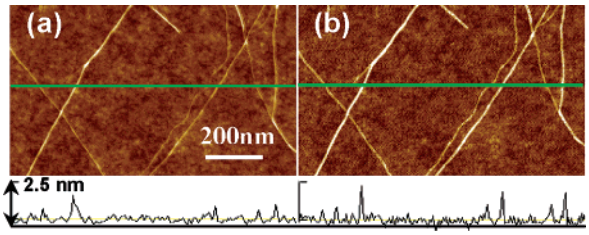

Figure 1. AFM images of SWNTs (a) before and (b) after rt plasma treatment. Bottom: topography height profiles along the green lines in the images.

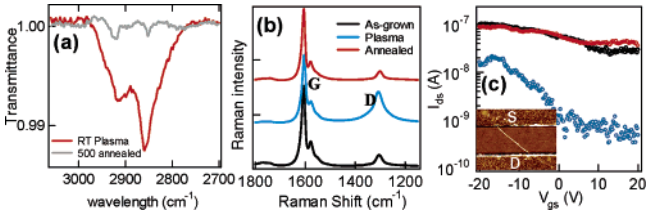

Figure 2. (a) IR and (b) Raman spectra of SWNTs before and after rt plasma treatment and after annealing. (c) Current−gate voltage ($I_{ds}-V_{gs}$) characteristics of an SWNT device before (black) and after rt plasma treatment (blue) and after 500 °C annealing (red). Bias = 10 mV. Inset shows the AFM image of the device with a nanotube bridging source−drain (S−D).

that dehydrogenation starts at ~200 °C and completes at ~500 °C (Figure 2a) likely via hydrogen release. This indicates the existence of $C-H_x$ species with different C−H bond strengths due to inhomogeneities in the SWNTs including different diameters.[8]

Raman spectroscopy measurements reveal that after rt H-plasma treatment, the ratio between the integrated area of disordered peak (D peak) and graphitic peak (G peak) (D/G) increases from 16% to 91% (Figure 2b). Hydrogenation causes sp^3 $C-H_x$ formation, introduces disorder on SWNT sidewalls, and thus increases the D band intensity. Upon annealing at 500 °C, the D/G ratio reduced to 19% (Figure 2b), suggesting dehydrogenation and recovery of the SWNT structures. Hydrogenation and annealing may have removed certain imperfections in the SWNTs.

Next, we carried out electrical transport measurements of individual SWNTs (see Supporting Information) to glean the effect of hydrogenation to the electrical properties. With over 100 single tube devices investigated, we consistently observed drastic conductance decreases after rt H-plasma treatment and nearly full recovery of the conductance after 500 °C annealing (Figure 2c). The conductance decrease upon hydrogenation can be attributed to the sp^2-sp^3 structure change of an SWNT, leading to localization of π-electrons. It was suggested that hydrogenation could open up or increase the band gap of SWNTs.[6] Accompanied by large decreases in the overall conductance, we indeed observed that the conductance of metallic and quasi-metallic SWNTs exhibited stronger gate−voltage dependence upon hydrogenation (Figure 2c). This was likely due to the more semiconducting nature of hydrogenated tubes.

10.1021/ja061324b CCC: $33.50

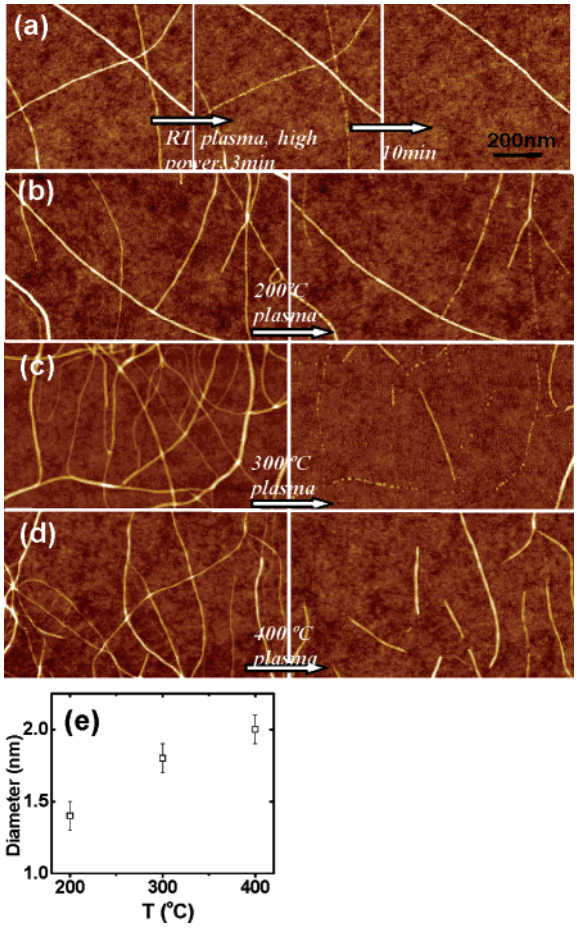

Figure 3. (a−d) AFM images of four SWNT samples before and after H-plasma treatment under various conditions. For (a), rf power is 50 W. For (b−d), rf power is 30 W and H-plasma is 3 min. (e) Diameter of the smallest tubes that "survived" H-plasma (30 W, 3 min) at various *T*.

The microscopy, spectroscopy, and electrical data above suggest that under the specific rt remote-plasma condition (30 W for 3 min), hydrogenation of SWNTs leads to structural and property changes that are largely reversible via dehydrogenation at 500 °C. However, under harsher plasma conditions at rt (i.e., higher power, such as 50 W, and longer plasma time up to 10 min), we observed irreversible etching and even complete removal of SWNTs especially for those with smaller diameters imaged by AFM (Figure 3a). Increasing the sample temperature from rt up to 400 °C during the 30 W/3 min plasma exposure also led to cutting and etching of SWNTs (Figure 3b−3d). These findings suggest that denser H-plasma and higher reaction temperatures can etch and completely remove SWNTs likely via gasification of nanotubes to hydrocarbon molecules (hydrocarbonation).

Our AFM results (Figure 3) combined with IR data (Supporting Information) reveal that, for high-temperature H-plasma treatment of SWNTs up to 400 °C (below the dehydrogenation *T* of ∼ 500 °C), H-etching and -cutting are accompanied by hydrogenation of SWNTs with the existence of $C-H_x$ species on the nanotubes (Figure 4b). These species vanish upon thermal annealing at 500 °C (Supporting Information), leaving the nanotubes in a cut and dehydrogenated form.

A noteworthy phenomenon observed during high temperature H-plasma treatments of SWNT is that smaller diameter nanotubes are H-etched and -cut more easily than larger tubes. We observed complete removal of SWNTs with diameters ≤ ∼1 nm by H-plasma treatment at 200 to 400 °C (Figure 3b−3d). If we define "surviving"

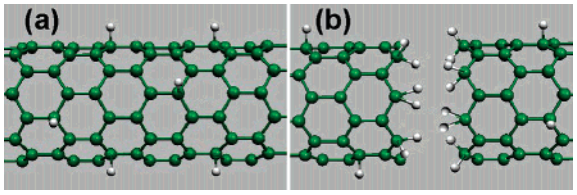

Figure 4. Schematic drawing of (a) hydrogenation and (b) hydrogenation plus etching of SWNTs by H-plasma at elevated temperatures (200−400 °C) or harsh plasma conditions at room temperature.

SWNTs as those with no visible cuts over ≥∼500 nm length under AFM, the diameters of the smallest "surviving" SWNTs exhibit a clear increasing trend under higher treatment temperatures (Figure 3e). That is, only larger SWNTs can survive higher temperature H-treatment. These results suggest higher reactivity of SWNTs with smaller diameters toward hydrocarbonation, due to the higher curvature and strain in the structures (similar to diameter dependent oxidation[9]). Calculations have predicted that smaller diameter SWNTs should exhibit higher hydrogenation reactivity due to higher curvature[8] but no theory exits for hydrocarbonation.

Dense and small cuts are typically observed along SWNTs with diameters in the range ∼1 to 1.5 nm after H-treatment at 200 °C and 300 °C (Figure 3b, 3c). This result suggests that relatively small nanotubes are attacked and cut nondiscriminately at dense sites along their lengths. These tubes are completely removed when H-plasma treated at ≥400 °C. For larger nanotubes (diameter > ∼1.7 nm), treatment by H-plasma at ≥400 °C causes fewer and wider cuts (Figure 3d), suggesting that H-etching of large nanotubes at high temperature likely starts at defect sites (or strained curved sites due to pinning interaction of the substrate) and then propagates along the tube length.

In summary, we have revealed structural enlargement, drastically reduced electrical conductance, and an increased semiconducting nature of SWNTs upon sidewall hydrogenation (Figure 4a) at room temperature. These changes are reversible upon thermal annealing at 500 °C via dehydrogenation. Harsh plasma or high temperature reactions lead to etching of nanotubes (Figure 4b), and smaller SWNTs are markedly less stable against hydrocarbonation than larger tubes. Our results are fundamental and may have implications to various applications including hydrogen storage, sensing, band gap engineering for novel electronics, and new methods of manipulation, functionalization and etching, and selection of nanotubes based on diameter.

Acknowledgment. This work was partially supported by Stanford GCEP and Intel.

Supporting Information Available: Experimental details. This material is available free of charge via the Internet at http://pubs.acs.org.

References

(1) Dai, H. *Surf. Sci.* **2002**, *500*, 218.
(2) Khare, B. N.; Meyyappan, M.; Casell, A. M.; Nguyen, C. V.; Han, J. *Nano Lett.* **2002**, *2*, 273.
(3) Nikitin, A.; Ogasawara, H.; Mann, D.; Denecke, R.; Zhang, Z.; Dai, H.; Cho, K.; Nilsson, A. *Phys. Rev. Lett.* **2005**, *95*, 225507.
(4) Zhang, G. Y.; Mann, D.; Zhang, L.; Javey, A.; Li, Y. M.; Yenilmenz, E.; Wang, Q.; McVittie, J.; Nishi, Y.; Gibbons, J.; Dai, H. *PNAS* **2005**, *102*, 16141.
(5) Kong, J.; Soh, H.; Cassell, A.; Quate, C. F.; Dai, H. *Nature* **1998**, *395*, 878.
(6) Park, K. A.; Seo, K.; Lee, Y. H. *J. Phys. Chem. B* **2005**, *109*, 8967.
(7) Heitz, T.; Drevillon, B.; Godet, C.; Bouree, J. E. *Phys. Rev. B* **1998**, *58*, 13957.
(8) Park, S.; Srivastava, D.; Cho, K. *Nano Lett.* **2003**, *3*, 1273.
(9) Zhou, W.; Ooi, Y. H.; Russo, R.; Papanek, P.; Luzzi, D. E.; Fischer, J. E.; Bronikowski, M. J.; Willis, P. A.; Smalley, R. E. *Chem. Phys. Lett.* **2001**, *350*, 6.

JA061324B